Supporting Information

Operando Raman and *ex situ* characterization of an iron-based conductive MOF as a negative electrode in Li-ion batteries

Isabel Ciria-Ramos[a,b], Alex R. Neale[c], Laurence J. Hardwick[c], Emilio J. Juarez-Perez[a,d], Ignacio Gascón [a,b,*] and Marta Haro[a,b,*]

[a] Instituto de Nanociencia y Materiales de Aragón (INMA), CSIC-Universidad de Zaragoza, Zaragoza, 50009, Spain

[b] Departamento de Química Física, Facultad de Ciencias, Universidad de Zaragoza, Zaragoza, 50009, Spain

[c] Stephenson Institute for Renewable Energy (SIRE) and the Department of Chemistry, University of Liverpool, Liverpool L69 7ZF, United Kingdom

[d] Aragonese Foundation for Research and Development (ARAID). Government of Aragon, Zaragoza, 50018, Spain

[*]mharo@unizar.es; igascon@unizar.es

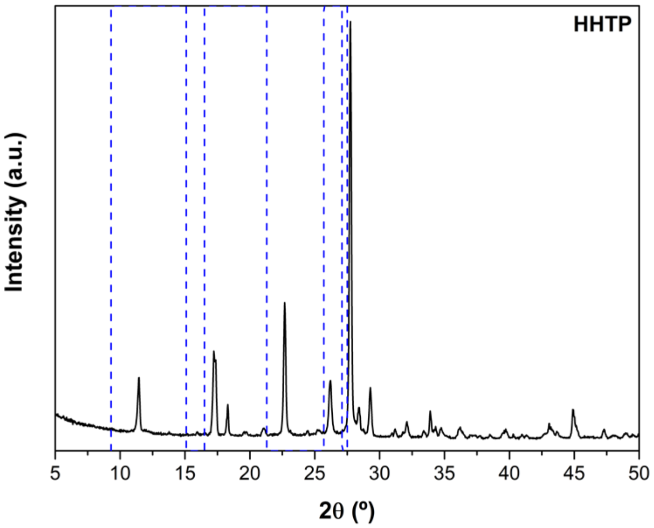

Figure S1. PXRD of the ligand HHTP indicating with blue dashed lines the positions at which Fe-HHTP peaks appear.

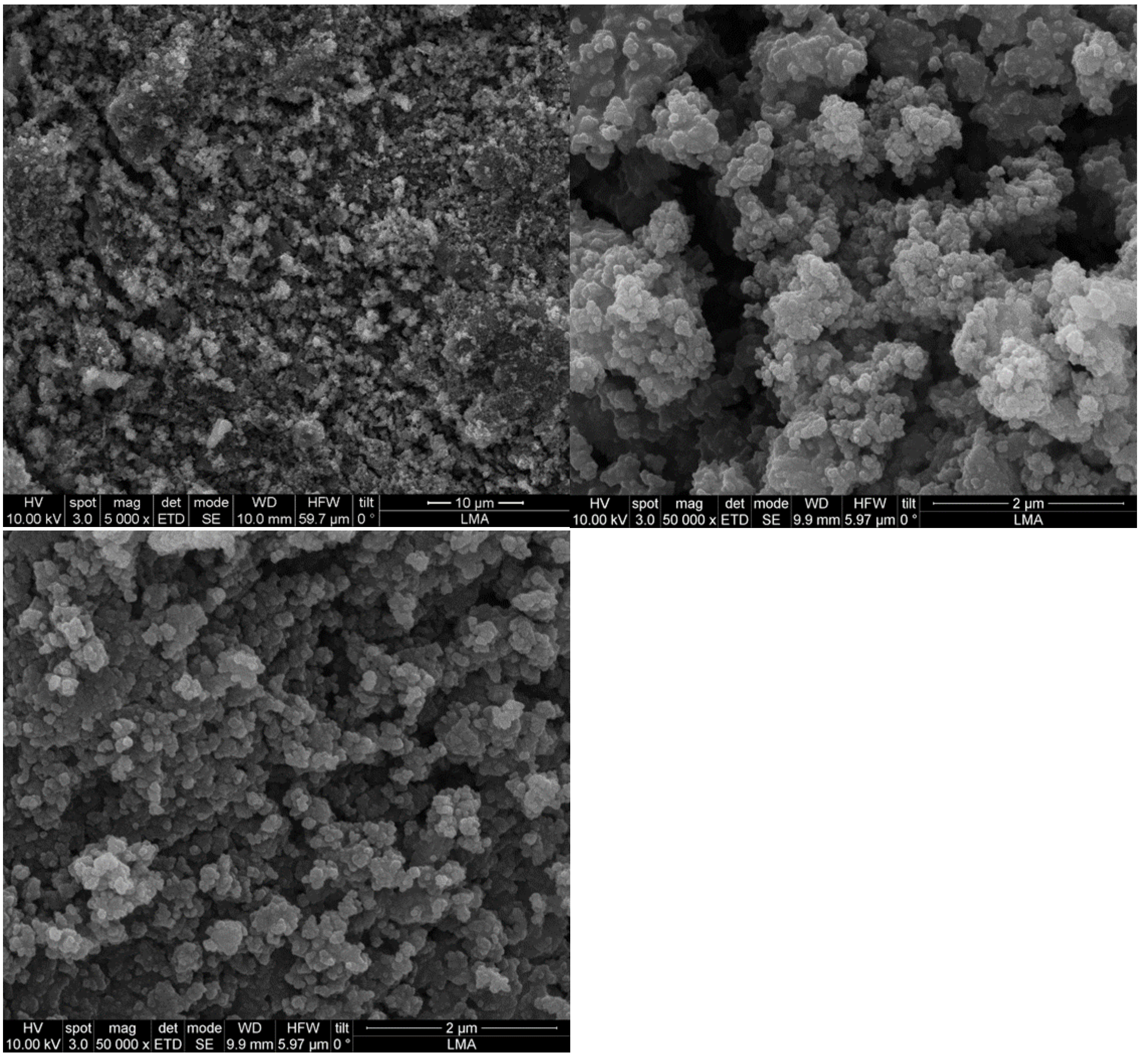

Figure S2. SEM images of the synthesized Fe-HHTP powders.

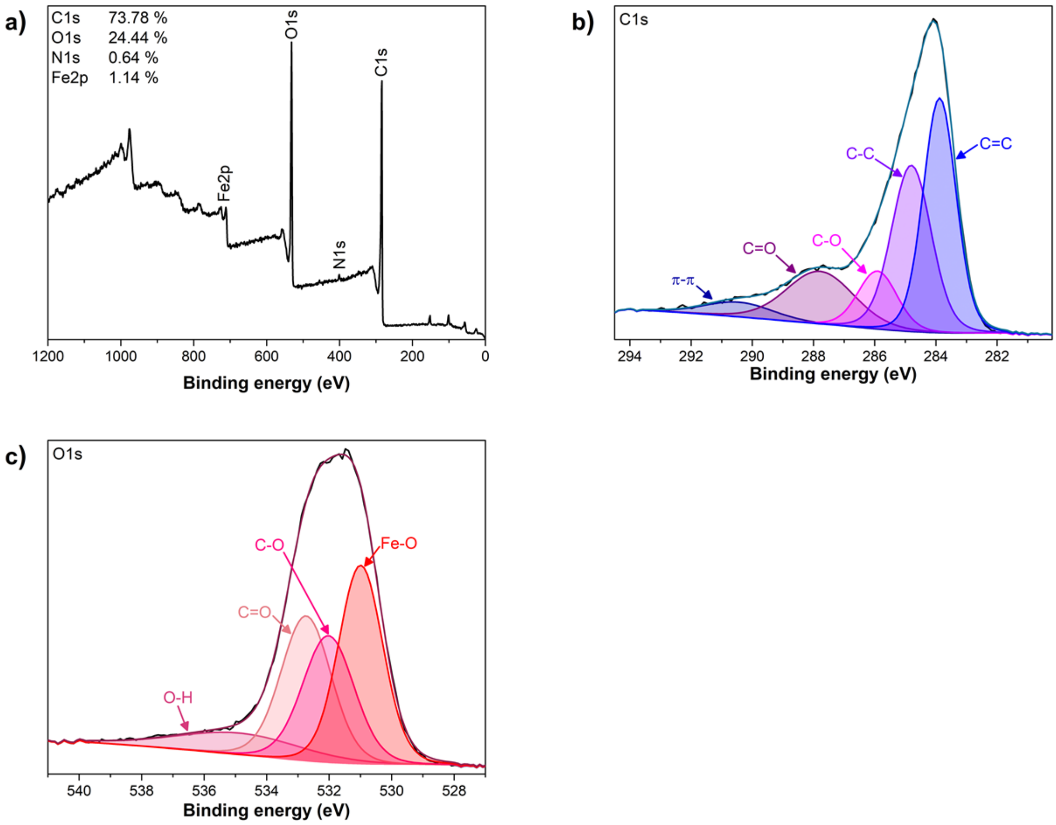

Figure S3. XPS of the synthesized MOF Fe-HHTP showing **a)** the survey, and the high-resolution **b)** C1s and **c)** O1s spectra.

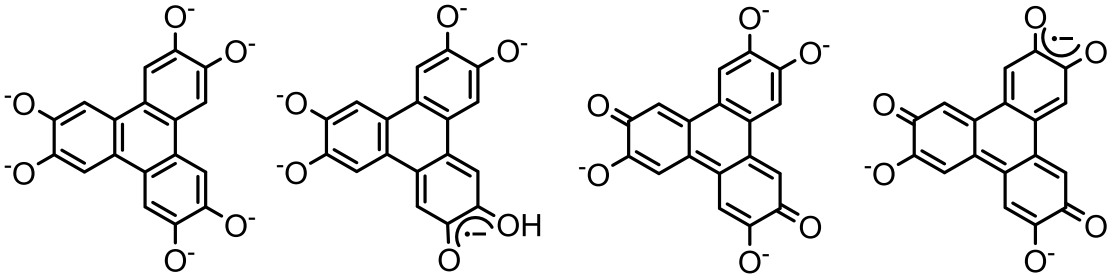

[cat, cat, cat]$^{6-}$ [cat, cat, sq]$^{5-}$ [cat, sq, sq]$^{4-}$ [sq, sq, sq]$^{3-}$

Figure S4. Configurations that can be adopted by HHTP in this study.

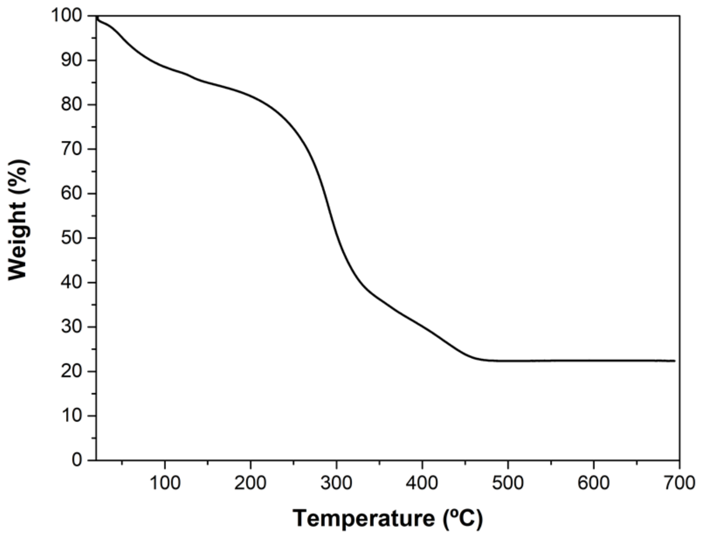

Figure S5. TGA graph of the synthesized Fe-HHTP powders.

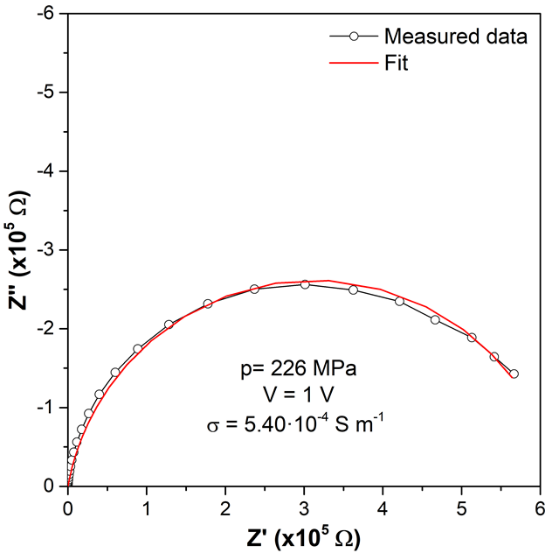

Figure S6. EIS spectra of the synthesized Fe-HHTP powders measured while applying a pressure of 226 MPa and a voltage of 1V.

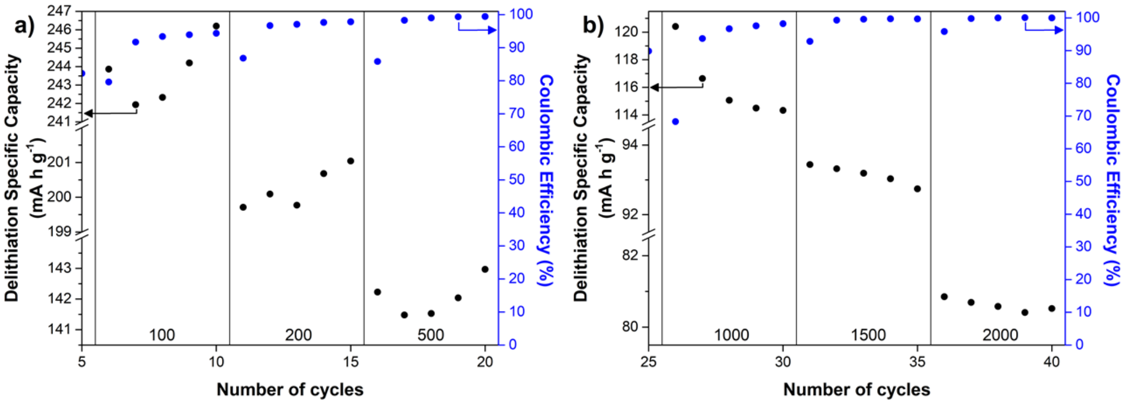

Figure S7. Close view of the delithiation specific capacities and the Coulombic Efficiencies of the rate capability graph shown in Figure 2 d) at **a)** low applied current rates (100 mA g^{-1}, 200 mA g^{-1} and 500 mA g^{-1}) and **b)** high applied current rates (1000 mA g^{-1}, 1500 mA g-1 and 2000 mA g^{-1}).

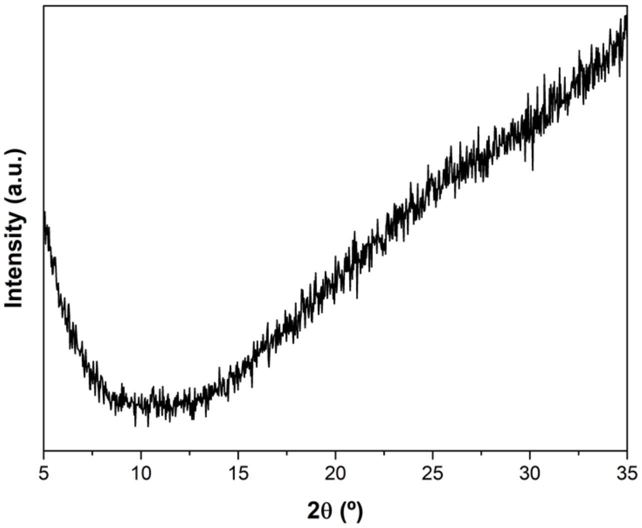

Figure S8. XRD of a fresh Fe-HHTP electrode.

No information of the MOF structural changes with cycles can be obtained by XRD since even the fresh electrode do not give rise to any discernible peaks in the XRD spectrum, probably because of the poor crystallinity of the initial material.

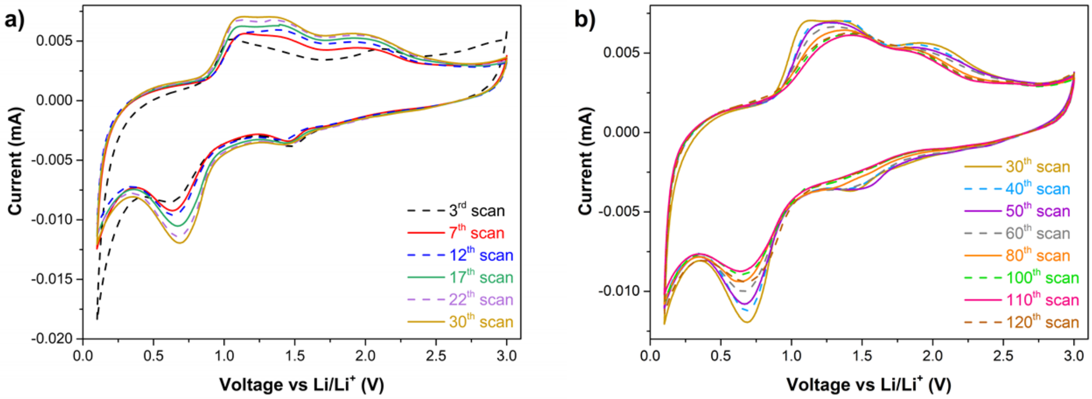

Figure S9. CVs obtained at a scan rate of 0.1 mV s^{-1} showing **a)** the initial 30 cycles and **b)** from cycle 30 to 125.

In the first 30 cycles, C-O cathodic peak intensity firstly slightly decreases and then fluctuates (Figure S9 a)). Regarding anodic peaks, the shoulder at ~0.3 V increases in the first cycles but then it becomes roughly constant, while C=C and C=O continuously evolves with scans. The former shifts to higher voltages in the initial 30 cycles and appears to divide into two broad peaks, as if the cleavage of C-Li and recovery of C=C bonds occurred simultaneously in the first cycles but eventually this reaction happens in a two-step process, probably due to kinetic reasons. Whereas the latter moves to lower voltages with cycles and becomes wider, indicating a more reversible cat ↔ sq reaction, being the sq formation the slowest process. Further cycling of the electrode leads to a shift to higher voltages of the peak associated to C-Li cleavage until it merges with the C=C formation one, and this unique peak gradually decreases its intensity (Figure S9 b)). Probably this is related to the non-recovery of C=C observed in XPS and ATR-FTIR. The intensities of cathodic C-C and anodic C=O peaks also decrease while the C-O formation peak disappears, probably indicating that the fully activation of the electrode requires less scans within these conditions (CVs with EIS measurements, ~30) than in galvanostatic cycles (225).

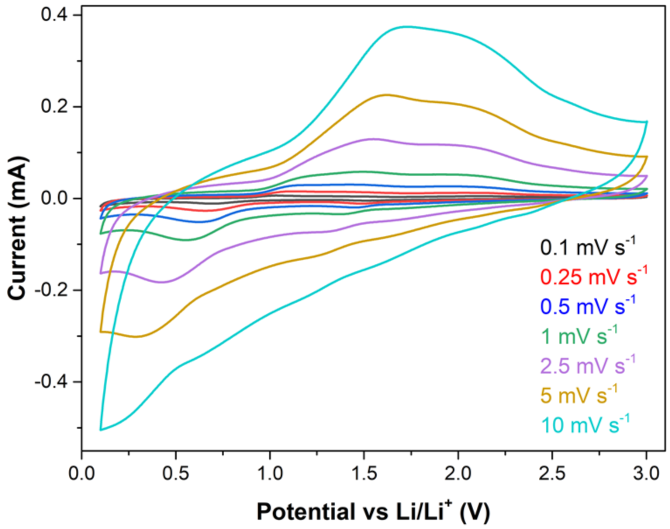

Figure S10. Graph displayed in Figure 6 b) showing the third scan of the CVs measured at scan rates from 0.1 mV s^{-1} to 10 mV s^{-1}.

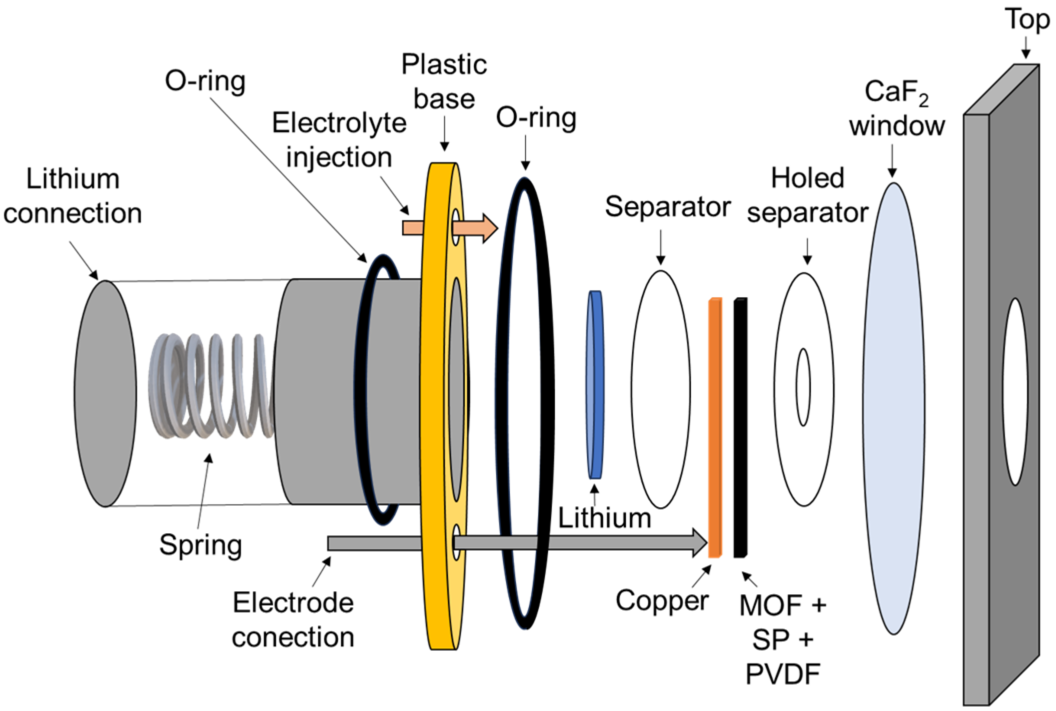

Figure S11. Configuration of the Raman cell employed for performing the *operando* Raman measurements.

Table S1. Raman peaks of dried Fe-HHTP powders and their corresponding assignments.

Raman shift (cm^{-1})	**Assignment**	**Reference**
215	Fe-HHTP (νFe-O)	[1]
280	Fe-HHTP (νFe-O)	[1]
395	Fe-HHTP (νFe-O + FeOOCC ring deformation)	[2]
492	Fe-HHTP (FeOOCC ring deformation)	[2]
589	Fe-HHTP (νFe-O)	[3,4]
642	Fe-HHTP (νFe-O)	[3,4]
1050	HHTP (δCH)	[3,5]
1345	HHTP (breathing mode)	[6]
1462	HHTP (catecholate) (νCC + δCH)	[3]
1575	HHTP (νCC)	[6]
2780	Overtone (analogue of 2D band)	[7]

References

1 D. L. A. De Faria, S. Venâncio Silva and M. T. De Oliveira, *J. Raman Spectrosc.*, 1997, **28**, 873–878.

2 J. Fujita, A. E. Martell and K. Nakamoto, *J. Chem. Phys.*, 1962, **36**, 324–331.

3 W. J. Barreto, R. A. Ando, P. S. Santos and W. P. Silva, *Spectrochim. Acta - Part A Mol. Biomol. Spectrosc.*, 2007, **68**, 612–618.

4 I. Michaud-Soret, K. K. Andersson, L. Que Jr and J. Haavik, *Biochemistry*, 1995, **34**, 5504–5510.

5 L. Öhrström and I. Michaud-Soret, *J. Phys. Chem. A*, 1999, **103**, 256–264.

6 A. Ferrari and J. Robertson, *Phys. Rev. B - Condens. Matter Mater. Phys.*, 2000, **61**, 14095.

7 C. Guo, Z. Li, F. Duan, Z. Zhang, F. Marchetti and M. Du, *J. Mater. Chem. B*, 2020, **8**, 9951–9960.